

# Effect of Green Plasticizer on the Performance of Microcrystalline Cellulose/Poly(lactic acid) Biocomposites

Uttam C. Paul, Despina Fragouli, Ilker S. Bayer, Arkadiusz Zych, and Athanassia Athanassiou\*

Cite This: *ACS Appl. Polym. Mater.* 2021, 3, 3071–3081

Read Online

ACCESS |



Metrics &amp; More



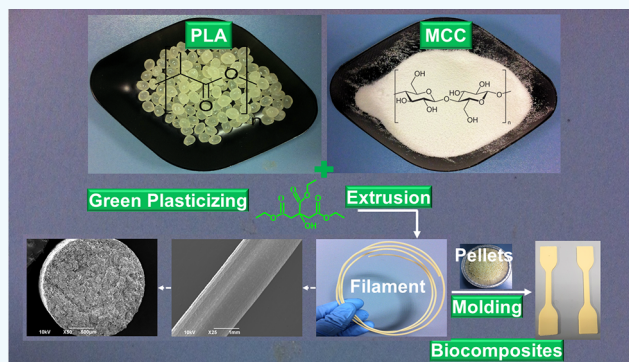
Article Recommendations



Supporting Information

**ABSTRACT:** In this study, we present the development of eco-friendly biocomposites composed of poly(lactic acid) (PLA) and microcrystalline cellulose (MCC), using melt extrusion and compression molding processes. In all the studied samples, the PLA/MCC ratio was always 1:1, whereas the plasticizer triethyl citrate (TEC) was responsible for the improved dispersion of the MCC in PLA. Tensile tests proved that the developed biocomposites containing TEC show improved ductility and crystallinity, as confirmed by the X-ray diffraction (XRD) study. Furthermore, the water vapor and oxygen permeability of the biocomposites were found to decrease as the TEC content increases in the formulation. Nonetheless, migration analyses to a dry food simulant prove that the migration of TEC is slightly above the acceptable limits when biocomposites with 15 wt % TEC were used. Taking this into account, in combination with the ranking of all the developed biocomposites according to their performance through the technique for order of preference by similarity to ideal solution (TOPSIS) analysis, we concluded that the PLA/MCC samples with 10 wt % TEC can be considered the most suitable biocomposites for eco-friendly food packaging applications. These findings place the developed PLA/MCC biocomposites among the strong candidates for biobased food packaging materials able to be produced at a large scale following industrially applicable methods since they are cost-effective and have improved properties compared to the pure biopolymer.

**KEYWORDS:** biocomposites, microcrystalline cellulose, PLA, water/oxygen barrier properties, packaging



## 1. INTRODUCTION

The continuously increasing number of human inhabitants on Earth impels the intensified production of consumption goods, which leads unavoidably to the generation of millions of tons of wastes. Possibly, the most voluminous and recalcitrant of all these wastes are fossil-fuel-based plastics. For this reason, in the last decades, a great part of the scientific community has focused its efforts on the development of new, cost-effective, and eco-friendly polymers and polymer composites from renewable, natural sources, targeting the replacement of petroleum-based products.<sup>1–4</sup> Despite their great abundance and sustainability, polymers from renewable, natural resources present diverse drawbacks in terms of performance and production costs, compared to some synthetic counterparts. The usual weak points of the bio-originating polymers are their poor mechanical properties, hydrophilicity, and difficult processability.

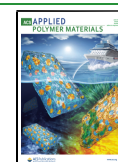
An excellent alternative to petroleum-derived polymers in terms of performance and costs is the poly(lactic acid) (PLA) biopolymer, mostly used in the packaging industry.<sup>1,5–8</sup> Despite its strong points, like being eco-friendly, having high tensile strength and stiffness and being biodegradable,<sup>7,9</sup> PLA is brittle, has low heat deflection temperature, and low thermal

stability during processing. Such constraints, in combination with the so-far limited supply, induce great limitations for its large-scale use in flexible packaging. To overcome these problems, diverse research efforts have focused on the combination of PLA with other materials,<sup>10–22</sup> such as natural fibers,<sup>10,23–25</sup> activated biochar,<sup>26</sup> microcrystalline cellulose (MCC),<sup>11–13,27</sup> and nanocellulose,<sup>14,15,28,29</sup> or blending PLA with other biodegradable polymers, such as natural rubbers,<sup>16,17</sup> thermoplastic polyurethane and elastomers,<sup>18–20</sup> polyhydroxyalkanoates (PHA),<sup>21</sup> polycarbonate (PC),<sup>22</sup> poly(butylene succinate),<sup>30</sup> and poly(butylene succinate-co-adipate).<sup>10,30</sup> Additionally, to form highly flexible materials with ideal properties for food packaging, PLA and PLA blends have been combined with numerous plasticizers such as poly(ethylene oxide) (PEO), polyethylene glycol (PEG), triethyl citrate (TEC), tributyl citrate (TBC), acetyl-tributyl citrate

Received: February 26, 2021

Accepted: May 10, 2021

Published: May 19, 2021



(TBAC), or epoxidized vegetable oils.<sup>31–36</sup> Among them, citrate ester-based plasticizers are widely used because of their good miscibility with the PLA and their biocompatibility, ideal for food contact applications.<sup>32,34,37</sup> Specifically, to improve the mechanical properties of the PLA, TEC, a nontoxic, eco-friendly, and natural plasticizer, has been widely used.<sup>37–42</sup>

In recent years, natural cellulosic fibers have been combined with polymers for the production of low-cost and high-performance materials. Cellulose is a low-cost, biocompatible, and biodegradable natural polymer that comes from abundant renewable sources with many favorable features such as high strength and stiffness and abundant hydroxyl groups available for various chemical modifications.<sup>10,43</sup> All these characteristics, as also the high specific surface area and adequate crystallinity of MCC, make it a promising cellulosic component for the reinforcement of polymer composites.<sup>4,9,12,43–45</sup> In fact, the combination of MCC with thermoplastic materials, such as PLA, makes the developed biocomposites ideal for the production of biodegradable products,<sup>11,13</sup> with improved dimensional, thermal stability, heat resistance, and also mechanical properties.<sup>46</sup> However, for large-scale applications, with industrial melt mixing methods like extrusion, injection molding, etc., that are used for the formation of the plastic materials, these systems are facing serious problems mainly due to the formation of strong agglomerates.<sup>13,47</sup> Consequently, this poor miscibility of MCC and PLA polymer melt makes the use of large quantities of this filler for large-scale production challenging.<sup>1,13,47</sup>

To the best of our knowledge, until now, for published studies on the development of MCC/PLA biocomposites, the MCC content does not exceed 25 wt % to the PLA.<sup>4,9,48–53</sup> For the improvement of the dispersion of MCC in PLA and, therefore, for the enhancement of the processability and commercial viability of the PLA/MCC biocomposites for flexible packaging applications, the interfacial interactions between these two components need to be improved. For this purpose, the surface silanization of MCC by 3-aminopropyltriethoxysilane (APS),<sup>52</sup> graftings of L-lactic acid,<sup>54</sup> and the surface acylation of MCC by acetyl chloride<sup>13</sup> have been used.

The goal of the current study is to develop PLA/MCC biocomposites with the highest possible MCC content concerning the bioplastic. On the basis of the preliminary extrusion experiments, we established that the maximum MCC amount that can be extruded with PLA is 50 wt %. Above which, the extrusion is not possible due to a high torque and filament braking. Subsequently, we optimized the TEC plasticizer concentration by keeping the PLA/MCC ratio at 1:1 and increasing the TEC content. TEC promotes a uniform blending of the high quantity of MCC with the PLA by plasticizing PLA, increasing the compatibility between the composite components and, therefore, preventing the aggregation of the MCC.

The food migration analysis shows that the overall TEC migration is in the range of tens of mg/dm<sup>2</sup>, although the acceptable daily intake (ADI) for humans of TEC is not limited (21CFR 184.1911). At the same time, the developed biocomposites present good mechanical, thermal, water, and oxygen barrier properties, all required in packaging applications, offering the possibility to replace, in some cases, fossil-based plastics or products made of PLA. All the developed biocomposites are compared and ranked following the technique for order of performance by similarity to ideal

solution (TOPSIS) analysis on the basis of the water vapor, oxygen barrier, mechanical, and migration properties to select the best biocomposite for food packaging applications.

## 2. EXPERIMENTAL SECTION

**2.1. Materials and Methods.** The commercial PLA (pellets diameter, 3–4 mm; density, 1.24 g/cm<sup>3</sup>; average molecular weight, 150 kDa; melting temperature, 145–160 °C; Ingeo 2003D, NatureWorks, Minnetonka, MN) was purchased from Sigma-Aldrich. PLA is semicrystalline with relatively slow nucleation and crystallization rates and is intended for fresh food packaging use. Triethyl citrate (TEC, Mw: 276.3 g/mol) and microcrystalline cellulose (MCC) in the form of white crystalline powder (density: 0.6 g/mL) were purchased from Sigma-Aldrich and were used as received. The MCC particle size ranges from 100 to 150 μm as the scanning electron microscopy (SEM) study in Figure S1a of the Supporting Information confirms.

**2.2. Pretreatment of PLA.** The PLA pellets were mechanically crushed using a dry mill IKA Pilotina MC machine (IKA-Werke GmbH & Co. KG, Staufen, Germany). The crushed PLA pellets were sieved with a 1.0 mm standard sieve at room temperature (RT) to select the PLA particles with sizes ranging from 900 to 1000 μm (the SEM image of the crushed PLA pellets is shown in Figure S1b, Supporting Information). This step was necessary for the uniform mixing of the two components (PLA and MCC) using a single feeder, twin-screw extruder.

**2.3. Preparation of Biocomposites.** At first, MCC and sieved PLA were dried at 50 °C in an oven for 24 h. For the preparation of all materials, (pure PLA, PLA/MCC biocomposites, and plasticized PLA and biocomposites (PLA/TEC and PLA/MCC\_TEC, respectively)) a twin-screw extruder (Scamex Rheoscam) was used (screw diameter, 20 mm; length to diameter ratio ( $L/D$ ), 20). The twin-screw extruder was operated at 75 rpm in all formulations. Before extrusion, the PLA, MCC, and TEC were premixed for about 15 min in a polyethylene bag by shaking. The PLA, PLA/TEC, PLA/MCC, and PLA/MCC\_TEC mixtures were extruded at 175 °C. The diameter of extruded filaments was ~1.75 mm, and the filaments were then cooled at RT. The biocomposites filament formulations and the sample codes are listed in Table 1.

**Table 1. Formulations of Prepared Biocomposites and Their Names<sup>a</sup>**

PLA (wt %)	MCC (wt %)	TEC (wt %)	final product name
100.0			PLA
95.0		5.0	PLA/5%TEC
90.0		10.0	PLA/10%TEC
85.0		15.0	PLA/15%TEC
50.0	50.0		PLA/MCC
47.5	47.5	5.0	PLA/MCC_5%TEC
45.0	45.0	10.0	PLA/MCC_10%TEC
42.5	42.5	15.0	PLA/MCC_15%TEC

<sup>a</sup>The wt % is with respect to the final composite.

The extruded filaments were then pelletized in pellets of ~4 mm diameter and dried at 50 °C overnight in an oven. To prepare the films, the pellets were compression molded using a CARVER hot press (Model 4122) at 175 °C for 5 min at contact pressure and then another 5 min at 5 MPa. Subsequently, a cooling step with running tap water through the platens of the hot press was performed. The resulting films were then stored for conditioning at 21 ± 2 °C and 50 ± 2% relative humidity (RH). The thickness of the films was determined by an electronic digital micrometer (Mitutoyo, 543–470B, sensitivity: 1 μm), measuring different regions of each sample, and an average of at least five measurements was calculated.

**2.4. Characterization.** **2.4.1. Scanning Electron Microscopy (SEM) Analysis.** The morphology of the biocomposites was investigated by a SEM microscope (Jeol JSM-6490LA, JEOL,

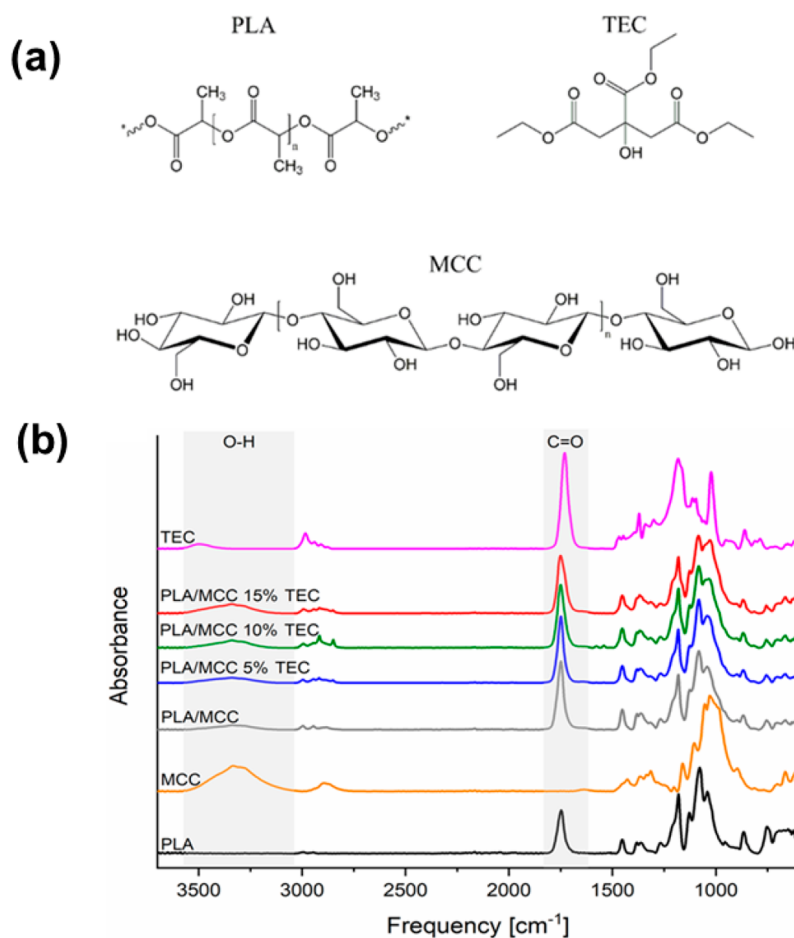


**Figure 1.** (a) Chemical structures of PLA, TEC, and MCC. (b) FTIR-ATR spectra of PLA, MCC, TEC, PLA/MCC, and PLA/MCC\_TEC biocomposites.

Tokyo, Japan). The microscope was equipped with a tungsten (W) thermionic electron source working in a high vacuum, and the acceleration voltage was 10 kV. For the analysis, the samples were fixed on aluminum stubs using carbon tape and a gold coating (thickness: 10 nm) was sputter-coated on each sample (Cressington 208 HR, high-resolution sputter coater). For the cross-sectional analysis, the specimens used for the mechanical properties analysis, after their fracture during the tensile testing, were used.

**2.4.2. Fourier Transform Infrared Spectroscopy-Attenuated Total Reflection (FTIR-ATR) Analysis.** The chemical compositions of all samples were investigated by FTIR-ATR (Vertex 70v equipped with an ATR unit: diamond crystal, Bruker Analytik GmbH). For each spectrum, 64 repetitive scans were averaged within the wavenumber range from 600 to 4000 cm<sup>-1</sup>, with a resolution of 4 cm<sup>-1</sup>.

**2.4.3. X-ray Diffraction (XRD) Analysis.** XRD measurements in a transmission geometry (TXRD) (Rigaku SmartLab X-ray powder diffractometer, Tokyo, Japan; operating at 40 kV and 150 mA; equipped with a rotating anode (9 kW Cu K $\alpha$ ) and a D\textit{e}X Ultra 1D silicon strip detector) were performed on dry MCC powder, as well as on PLA and all the biocomposite films, at ambient temperature.<sup>55</sup>

**2.4.4. Mechanical Properties Analysis.** The tensile testing measurements were conducted with an Instron dual column tabletop universal testing system (T.A. Instruments, Instron, Model 3365L4052, Norwood, MA) with a 2 kN load cell, following the ASTM D882 standard test methods for tensile properties of thin plastic sheeting at 25 °C. Specimens of about 550  $\mu$ m thickness were first conditioned for 48 h at standard laboratory conditions (i.e., 21  $\pm$  2 °C and 50  $\pm$  2% RH). Then, they were cut with a dog bone press (length of 35 mm, width of 4 mm) and were tested at a rate of 5 mm/min. From the obtained stress–strain curves, the Young’s modulus,

ultimate tensile strength, elongation at break, and toughness (area under the stress–strain curve) were calculated. For each biocomposite, five specimens were tested, and for each parameter, the mean value with the standard deviation was reported. To analyze the data, analyses of variance (ANOVA), using OriginPro 2018 software (Northampton, MA) was performed. The multiple-range Tukey’s test was used to compare the differences between the mean values of the measured properties (significance level: 0.05).

**2.4.5. Thermal Analysis.** The thermal stability of the films was characterized utilizing thermogravimetric analysis (TGA) with a Mettler Toledo thermogravimetric/differential scanning calorimetry (TGA/DSC) tester. Each sample (15–25 mg) was placed in a platinum pan, and the measurement was performed under a constant flow of nitrogen, with a heating rate of 10 °C/min, from 30 to 600 °C.

**2.4.6. Water Vapor Permeability Analysis.** The water vapor permeability (WVP) of the films was determined gravimetrically according to the standard method described elsewhere.<sup>56</sup> The tests were carried out in an in-house developed device at ambient temperature under 100% RH gradient ( $\Delta$ RH%).<sup>56,57</sup> The weight loss of permeation cells was plotted as a function of time. Then, the water vapor transmission rate (WVTR) was determined from the slope of each line obtained from the linear regression following the eq 1.

$$\text{WVTR (g/m}^2\cdot\text{day)} = \frac{\text{slope}}{\text{area of the film}} \quad (1)$$

For each film, the WVP measurement was repeated three times and the mean value with the standard deviation was reported. The WVP of the films was calculated as follows:<sup>57</sup>

$$\text{WVP} (\text{g}\cdot\text{m}/\text{m}^2\cdot\text{day}\cdot\text{Pa}) = \frac{\text{WVTR} \times l \times 100}{P_s \times \Delta\text{RH}} \quad (2)$$

where,  $l$  (m) is the mean film thickness,  $\Delta\text{RH}$  (%) is the percentage RH gradient, and  $P_s$  (Pa) is the saturation water vapor pressure at 25 °C.

**2.4.7. Water Contact Angle (WCA) Analysis.** The wetting characteristics of all samples were determined by WCA measurements using a contact angle goniometer, (DataPhysics OCAH 200, Kruss). Three microliters of water droplets was placed on the surfaces of the films, and the WCA measurements were performed within 30 s. At least 10 measurements were done for each sample in different areas, and the average values are reported with the standard deviation.

**2.4.8. Oxygen Permeability Analysis.** The oxygen permeability of the films was analyzed according to ASTM test method F 3136-15 (ASTM, 1989), using an Oxysense 5250i device (Oxysense) equipped with a film permeation chamber. The test was performed at ambient conditions ( $T = 21 \pm 2$  °C and  $\text{RH} = 50 \pm 2\%$ ). The permeation chamber consists of a cylinder divided into two parts (sensing well and driving well). At first, the sample was placed over the sensing well and the chamber was closed properly by using the locking bolts. The sensing well is equipped with a fluorescence sensor (oxidot) mounted on the nitrogen purged side of the chamber while the driving well is kept open to ambient air. The oxygen gas transmission rate (OTR) of the films was measured using the Oxysense permeability (OP) analyzer with a fluorescence sensor. When oxygen passes from the driving well through the films to the sensing well, the fluorescence is quenched, decreasing its lifetime proportionally to the oxygen concentration. The Oxysense software measures this oxygen concentration over time (OTR). For each sample, at least five recorded values were taken and the average values are reported with the standard deviation. Equation 3 was used to calculate the oxygen permeability (OP)

$$\text{OP} = \text{OTR} \times l \quad (3)$$

**2.4.9. Food Migration Analysis.** The food migration analysis was performed using the Tenax food simulant, following the method previously described.<sup>58,59</sup>

**2.4.10. Ranking of Biocomposites Using TOPSIS.** TOPSIS is a multicriteria decision-making (MCDM) tool<sup>60,61</sup> used to select the best biocomposite among all other biocomposites in this study. The TOPSIS methodology, equations, and decision matrix criteria are shown in the Supporting Information.

### 3. RESULTS AND DISCUSSION

**3.1. Chemical Analysis.** The chemical structures of PLA, TEC, and MCC are shown in Figure 1a, and the chemical compositions of the obtained biocomposite films were characterized by FTIR-ATR spectroscopy. As shown in Figure S2 and Table S1 and in Figure 1b, the FTIR-ATR analysis proves that all the blends of PLA/TEC as well as the PLA/MCC\_TEC biocomposites contain all claimed components and suggests that the materials did not degrade during the extrusion process. In particular, all films containing PLA show a characteristic peak around  $1750 \text{ cm}^{-1}$ , corresponding to the carbonyl stretching vibration ( $\nu\text{C}=\text{O}$ ) band of PLA. The carbonyl group of pure TEC shows maximum absorption at around  $1730 \text{ cm}^{-1}$ , and when TEC is combined with the PLA, it overlaps with the carbonyl absorption of PLA. All biocomposites containing MCC show also a broad peak with a maximum of around  $3340 \text{ cm}^{-1}$ , corresponding to the absorption of hydroxyl groups stretching vibrations ( $\nu\text{O}-\text{H}$ ).<sup>15</sup>

**3.2. Morphological Analysis.** The compression-molded biocomposite films made of PLA and MCC (1:1 ratio) without plasticizer macroscopically show a heterogeneous distribution of the components, appearing as surface defects or bumps

(Figure 2a). Microscopically, as revealed by the SEM analysis (Figure 2e), agglomerates of MCC appear on the surface of the

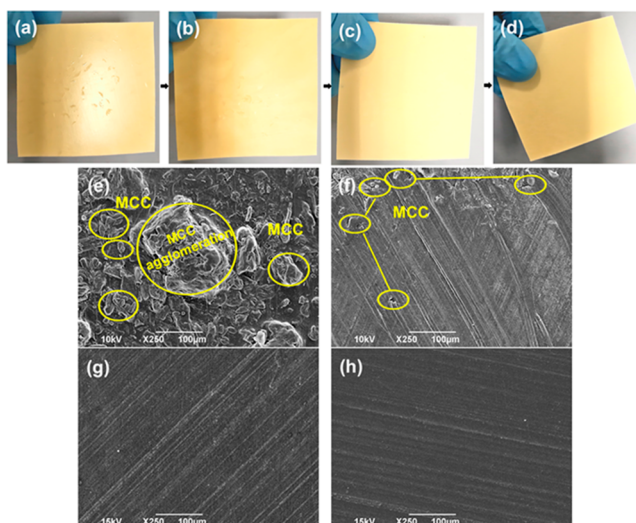


**Figure 2.** Photographs of extruded and hot pressed biocomposite films of (a) PLA/MCC, (b) PLA/MCC\_5%TEC, (c) PLA/MCC\_10%TEC, and (d) PLA/MCC\_15%TEC. SEM images of the surface morphology of (e) PLA/MCC, (f) PLA/MCC\_5%TEC, (g) PLA/MCC\_10%TEC, and (h) PLA/MCC\_15%TEC. Surface and cross-sectional morphology of PLA, and PLA/TEC films are shown in Figures S3 and S4.

biocomposites, indicating poor interfacial interaction between PLA and MCC. However, after the introduction of TEC, the compression-molded films appear homogeneous, the surface bumps almost disappear, and the samples become more ductile (Figure 2b–d,f–h). Due to its low molecular weight, TEC can easily penetrate to the interface of the biocomposite components, compatibilizing them, and in this way, the resulting films exhibit an overall smoother surface. These findings are in good agreement with those of Herrera et al.<sup>62</sup> and Qu et al.,<sup>63</sup> who have proven that TEC and PEG enhance the dispersion of chitin and cellulose nanofillers in the PLA matrix. To further support this statement, the SEM analysis of the cross-section of the biocomposites is presented in Figure 3 and Figures S3 and S4. In the case of PLA/MCC, the presence of large holes and extended fractures is evident (Figure 3a). The SEM micrographs of the cross-section of the films with TEC reveal that the introduction of TEC gradually improved the dispersion of the MCC in the PLA matrix. In particular, in Figure 3b–d, it can be seen that, in the presence of 5 wt % TEC, MCC agglomeration is still evident and the sample is brittle, as shown in Figure 5. This indicates that 5 wt % TEC is not enough to improve the dispersion of MCC in the PLA matrix. When the amount of TEC is increased to 10 wt %, the brittle-to-ductile transition of the sample occurred. This can be attributed to the better mixing/blending of PLA and MCC with TEC. Further, with an increase of the TEC concentration (15 wt %), the sample becomes more ductile. This is due to the plastification effect of a higher (15 wt %) amount of TEC (Figure S6, Supporting Information).

**3.3. Crystallographic Analysis.** As shown in the XRD analysis of Figure S5, the PLA films exhibit only a broad halo diffraction band at  $2\theta = 15.8^\circ$ , which suggests that the sample is amorphous,<sup>4,38</sup> while the introduction of up to 15 wt % TEC does not induce crystallization. On the contrary, the XRD

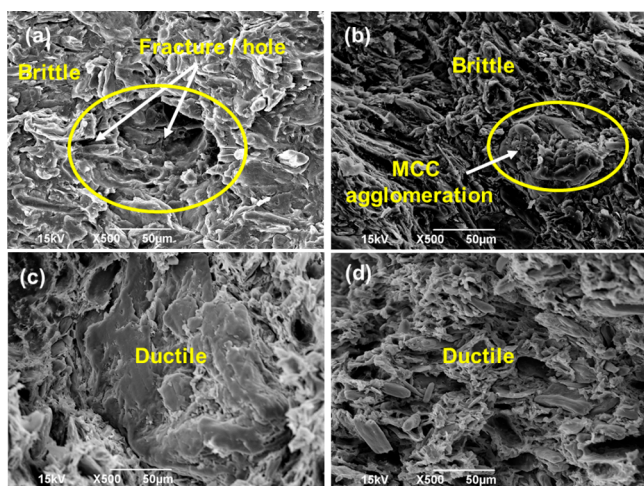


**Figure 3.** SEM cross sectional images of (a) PLA/MCC, (b) PLA/MCC\_5% TEC, (c) PLA/MCC\_10% TEC, and (d) PLA/MCC\_15% TEC biocomposites.

pattern of pure MCC shows diffraction peaks at  $2\theta = 15.2^\circ$ ,  $22.5^\circ$ , and  $34.5^\circ$ , revealing the crystalline nature of cellulose<sup>5,13</sup> (Figure 4). When PLA and MCC are combined, the XRD

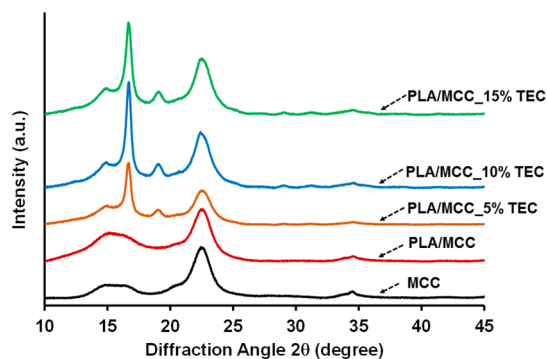


**Figure 4.** Diffraction patterns for MCC, PLA/MCC, PLA/MCC\_5% TEC, PLA/MCC\_10%TEC, and PLA/MCC\_15%TEC biocomposites.

pattern of the sample (PLA/MCC) shows the same peaks as the pure MCC, indicating that the presence of the PLA matrix does not affect the crystalline structure of MCC.<sup>5</sup> The crystalline structure of MCC is not affected also in the PLA/MCC\_TEC samples. However, in that case, the addition of TEC to the PLA/MCC biocomposites leads to the generation of two new distinct diffraction peaks located at about  $16.7^\circ$  and  $19.1^\circ$ . This is the most common and stable polymorph diffractogram of PLA  $\alpha$ -crystal.<sup>55</sup> Therefore, the plasticizing effect of TEC seems to induce the crystallization of PLA/MCC\_TEC biocomposites.<sup>4,6,42</sup>

**3.4. Mechanical Properties Analysis.** Figure 5a–e shows the results obtained after the tensile tests of different samples developed in this study. Pure PLA shows the tensile strength and Young's modulus of  $59.2 \pm 2.2$  and  $1555.8 \pm 54.5$  MPa, respectively. Regarding the elongation at the break, pure PLA shows a quite low value of  $5.7 \pm 0.5\%$ , which in the presence of MCC becomes even lower ( $2.0 \pm 0.1\%$ ), demonstrating the high rigidity of the PLA/MCC materials. This can be attributed to the brittle nature of PLA, which is further magnified by the poorly dispersed MCC, as also observed in

the SEM analysis (Figures 2 and 3). The plasticization effect of TEC is evident from the tensile stress–strain curves (Figure S6, Supporting Information). As shown in Figure 5a, the Young's modulus of both PLA and PLA/MCC remained almost unchanged with the addition of 5 wt % TEC; however, this dropped gradually when 10 and 15 wt % TEC were introduced. The ultimate strength follows a similar trend. The elongation at the break and the toughness of samples containing 10 wt % TEC are higher than those of pure PLA, confirming the plasticization effect of TEC. When the TEC amounts increased to 15 wt %, a sharp increase of elongation at break to  $595.4 \pm 27.2$  for PLA/15% TEC (from  $5.7 \pm 0.5$  for PLA) and  $299.8 \pm 9.8$  for PLA/MCC\_15% TEC (from  $2.0 \pm 0.1$  for PLA/MCC) as well as of the toughness to  $74.81 \pm 8.80$  for PLA/15% TEC (from  $2.2 \pm 0.3$  for PLA) and  $14.6 \pm 0.43$  for PLA/MCC\_15% TEC (from  $0.44 \pm 0.04$  for PLA/MCC) were observed. Due to the low molecular weight of the TEC plasticizer (276.3 g/mol), its molecules penetrate the interface between PLA and MCC, weakening the direct binding forces among the macromolecules. In this way, the molecular chains can easily slide and move upon stress, resulting in an increase of the strain at break<sup>4</sup> and a decrease of the stiffness. Therefore, the addition of TEC gradually increases the ability of the biocomposites to experience plastic deformation and at the same time decreases their stiffness, which are highly desirable properties for molding and shaping processes.<sup>64</sup> Figure 5e shows that the stress whitening zones appear near the fracture when a high elongation ( $299.8 \pm 9.8\%$ ) is achieved. We attribute the stress whitening to the debonding of MCC from the PLA matrix at this elongation and, as a consequence, the creation of voids that scatter light, making the sample appear white.<sup>4</sup> Therefore, the present results clearly show that PLA and PLA/MCC modified with TEC can overcome their intrinsic brittleness, resulting in a significant improvement of their ductility and toughness.

**3.5. Thermal Degradation Analysis.** The thermal degradation behavior of the biocomposites was investigated by TGA analysis, as shown in Figure 6. The neat PLA starts to decompose to volatile compounds at around  $300^\circ\text{C}$  with a maximum at  $362^\circ\text{C}$ , while for MCC, the maximum decomposition happens at  $328^\circ\text{C}$ . When these two materials are combined, two distinct decomposition temperatures, attributed to the two polymeric components, can be observed after the deconvolution of the PLA/MCC curve (Figure S7, Supporting Information). These two peaks confirm that there are no strong interactions upon simple mixing of the two polymers. However, the addition of TEC in the biocomposite formulation significantly improves the interaction between the polymers since, as shown in Figure 6b, only one degradation temperature appears with the value between the ones of the individual components (the degradation temperature of the biocomposites increases from  $338^\circ\text{C}$  for 5 wt % TEC to  $344^\circ\text{C}$  for 10 and 15 wt % TEC), confirming a good dispersion and compatibility. It should be mentioned that pure TEC starts to evaporate at around  $100^\circ\text{C}$  due to its relatively low boiling point of  $294^\circ\text{C}$ . However, the incorporation of TEC into the PLA matrix slows down the evaporation process and has no adverse effects on the decomposition of the PLA matrix both in the case of the PLA/TEC blends and PLA/MCC\_TEC biocomposites (Figure S8, Supporting Information).

**3.6. Water Vapor Permeability and Wetting Behavior Analysis.** The effect of TEC on the PLA matrix and their composites with MCC on the water barrier and wetting

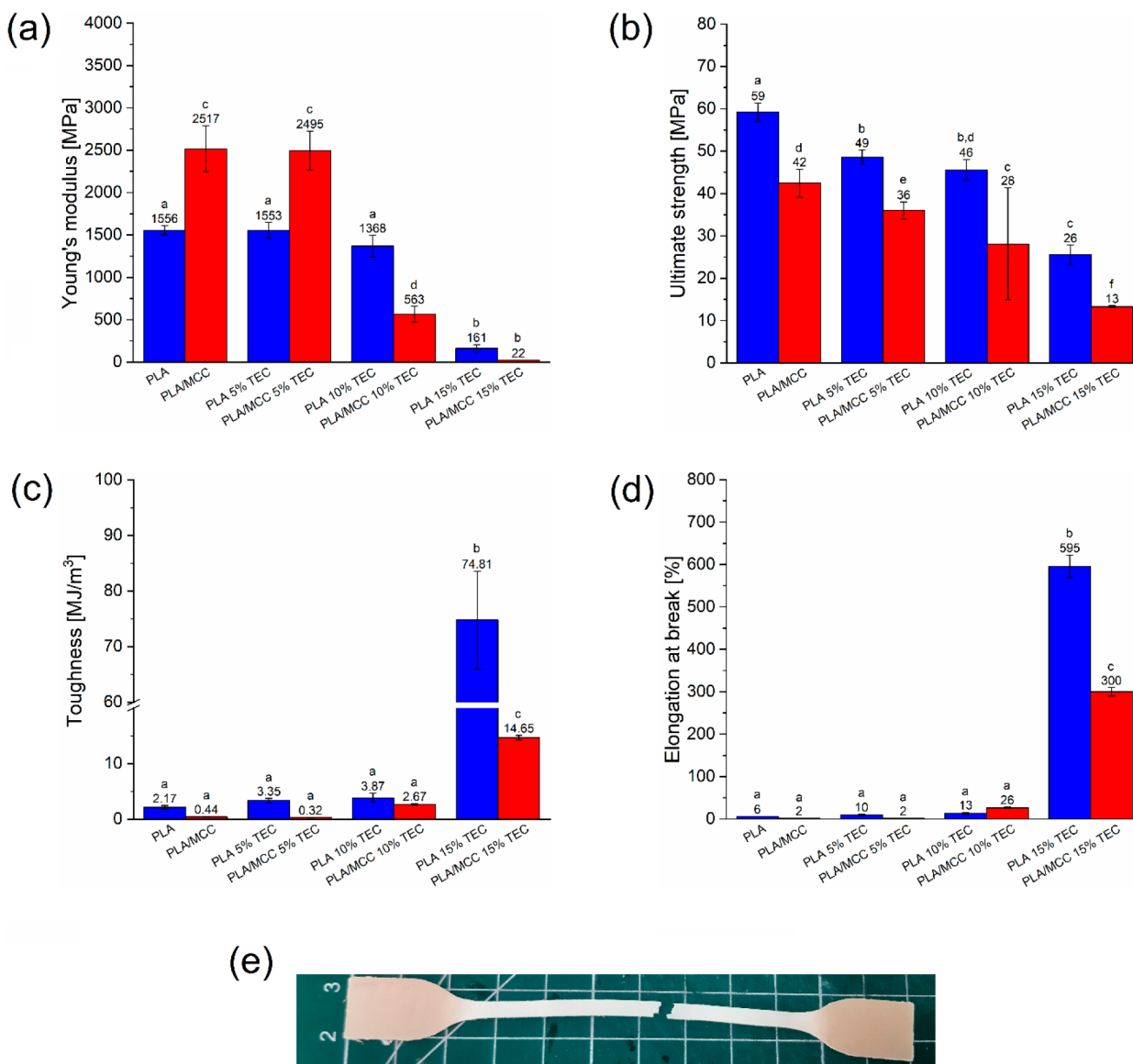


**Figure 5.** (a) Young's modulus ( $E$ ), (b) ultimate tensile strength (UTS), (c) elongation at break, and (d) toughness of PLA, PLA/TEC blend, PLA/MCC, and PLA/MCC\_TEC biocomposites. (e) PLA/MCC\_15% TEC after tensile test. Equal letters indicate no statistically significant differences ( $p \leq 0.05$ ) based on the ANOVA.

properties were investigated by the WVP, WCA, and moisture uptake analysis. As shown in Figure 7, the WVP of PLA film was found to be  $3.6 \times 10^{-5} \pm 4.2 \times 10^{-6} \text{ g}\cdot\text{m}/\text{m}^2\cdot\text{day}^{-1}\cdot\text{Pa}^{-1}$ . When PLA was plasticized with TEC, a significant decrease of the WVP of the PLA/TEC films by 88% for PLA/5%TEC, 95% for PLA/10%TEC, and 94% for PLA/15%TEC were observed, compared to that of PLA. When PLA is combined with MCC, the WVP values significantly increase to  $8.4 \times 10^{-5} \pm 1.1 \times 10^{-5} \text{ g}\cdot\text{m}/\text{m}^2\cdot\text{day}^{-1}\cdot\text{Pa}^{-1}$ . This may be attributed to the polar nature of MCC and its heterogeneous distribution in PLA, as also proven by the SEM analysis (Figures 2 and 3). However, when TEC was introduced in the biocomposites, the WVP values decreased to those for PLA/MCC. Decreases of 43%, 87%, and 78% for 5, 10, and 15 wt % TEC-containing composites were observed.<sup>65,66</sup> The WVP of diverse polymers widely used in packaging applications and their comparison with the herein developed biocomposites are shown in Table S8.

The WCA analysis of all the PLA/TEC and PLA/MCC\_TEC biocomposite films indicates no significant changes in the wettability of the developed materials. In particular, the WCA of pure PLA films is  $99.5 \pm 1.6^\circ$ , while the addition of 5 and 10 wt % TEC in PLA leaves the WCA practically unaltered (WCA  $98.5 \pm 5.2^\circ$ , for PLA/5%TEC and  $101.3 \pm 2.0^\circ$  for PLA/10%TEC). Only in the case of PLA/15%TEC, the WCA decreases slightly (WCA  $85.6 \pm 0.4^\circ$ ) probably due to the smoother surface of PLA/TEC films with a higher TEC content. Similar behavior was observed also for the PLA/MCC biocomposites, where the presence of TEC slightly decreases the WCA of the films. In particular, from  $98.0 \pm 1.2^\circ$  for PLA/MCC, the WCA becomes  $94.1 \pm 2.5^\circ$ ,  $86.9 \pm 2.0^\circ$ , and  $82.0 \pm 2.9^\circ$  for the biocomposites with TEC concentrations of 5, 10, and 15 wt % respectively. This can be attributed to the smoother surface of the biocomposites with increasing TEC content, as already proven by the SEM study and, therefore, to the lower number of air pockets trapped

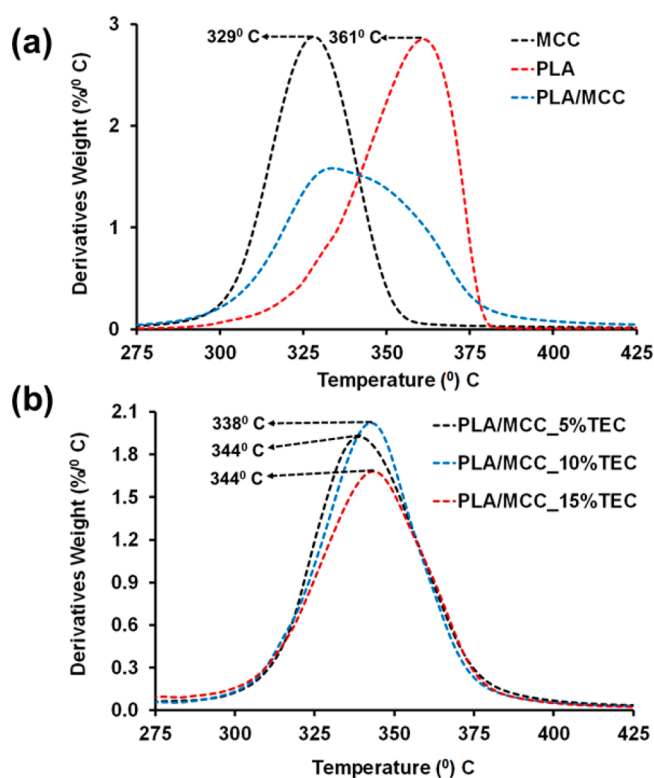


**Figure 6.** Thermal degradation behavior of (a) DTG of PLA, MCC, and PLA/MCC and (b) DTG of PLA/MCC\_TEC biocomposites.

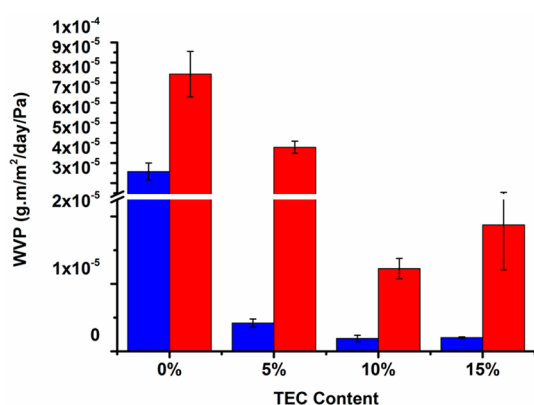


**Figure 7.** WVP values of PLA/TEC and PLA/MCC\_TEC biocomposites. The blue column is for PLA/TEC blends and their MCC-containing analogues (red column).

between the water droplet and the solid surface that usually contribute to the hydrophobicity of the rough surfaces according to the Cassie–Baxter law.<sup>67</sup> The dynamic water contact angle analysis further confirms that no significant WCA changes were noticed over the time for the biocomposite samples, as shown in Figure S9. After the storage of the biocomposites under 100% RH for 14 days (Figure S10, Supporting Information), the final moisture content (MC) of PLA/MCC was  $5.83 \pm 0.80\%$ , which is significantly lower than the corresponding value for pure MCC powder ( $15.95 \pm 1.36\%$ ) but higher than that of the pure PLA value ( $0.17 \pm 0.13\%$ ). When TEC was introduced to the biocomposites, the MC decreased slightly, reaching  $5.26 \pm 0.97\%$  for PLA/MCC\_5%TEC,  $5.52 \pm 0.23\%$  for PLA/MCC\_10%TEC, and  $4.59 \pm 0.37\%$  for PLA/MCC\_15%TEC. The latter MC value

is 27.02% lower compared to the one for PLA/MCC. This indicates that the decrease of the moisture content in PLA/MCC\_TEC biocomposites is solely attributed to the presence of TEC, which induces the good mixing and interaction of the two polymers. Therefore, the presence of the TEC in the biocomposites, apart from inducing a plasticizing effect to the biocomposites, provides better resistance against water and humidity.

**3.7. Oxygen Barrier Properties Analysis.** The OP properties of the fabricated films are illustrated in Figure 8a. The measured permeability value for PLA/TEC significantly increased at 5 wt % TEC and decreased when the amount of TEC was 10 and 15 wt % in PLA. In the biocomposites, the OP value of PLA/MCC significantly increased in comparison to that of pure PLA. This can be attributed to the heterogeneous distribution of MCC in PLA, which creates voids/holes in biocomposites, as also observed in the SEM (Figure 3). A similar situation was observed also for the PLA/MCC\_5%TEC biocomposite, indicating that 5 wt % TEC is not enough to improve the homogeneity and decrease the OP of the biocomposites. A significant OP decrease was observed when the amount of TEC was increased to 10 wt % (OP of PLA/MCC\_10%TEC is  $6.3 \pm 0.1 \text{ cm}^3 \cdot \text{mm} / \text{m}^2 / \text{day}$ ). The OP reduction in PLA/MCC\_10%TEC is around 75.8% compared to that of pure PLA and 99.7% compared to that of the PLA/MCC biocomposite. This can be attributed to the better mixing/blending of PLA and MCC with TEC, which induces higher tortuosity paths for the oxygen molecules and, therefore, causes the OP reduction of the film. A further increase of the TEC concentration (15 wt %) does not improve the oxygen barrier further (OP =  $18.9 \pm 1.5 \text{ cm}^3 \cdot \text{mm} / \text{m}^2 / \text{day}$ ). This increase is most likely attributed to the greater free volume throughout the composite matrix because of the plastification effect of a higher (15 wt %) amount of TEC (Figure 3 and Figure S6, Supporting Information), promoting an improved oxygen permeation without providing further improvement in the dispersion of MCC. However, this OP value still lower than that of neat PLA. The OP values in comparison with other commercial polymeric materials for packaging are shown in Figure S11. It should be highlighted that the OP value of PLA/MCC\_10%TEC is lower than those of other commercial products. On the basis of the obtained water and oxygen barrier values, it is possible to propose the use of developed biocomposites for peanuts, meats, and MAP packaging applications.<sup>68</sup>

**3.8. Overall Migration Analysis.** The overall migration test with a food simulant was carried out to investigate the possible migration of molecules from the biocomposites toward food. The test simulates food contact, by using the food simulants E, according to the current EU legislation (EU Commission Regulation No. 10/2011 for plastic materials and articles). The migration of components from the different biocomposites toward food was tested using Tenax as a dry food simulant. The results presented in Figure 8b show that the overall migration for PLA and PLA/5%TEC is negligible and that for PLA/10%TEC is about  $9.5 \pm 1.0 \text{ mg dm}^{-2}$ . For PLA/15% TEC, the overall migration reached  $45.1 \pm 3.7 \text{ mg dm}^{-2}$ . Similarly, for PLA/MCC, and PLA/MCC\_5% TEC, the migration is negligible and that for PLA/MCC\_10%TEC is about  $7.1 \pm 2.6 \text{ mg dm}^{-2}$ , while in the case of the PLA/MCC\_15%TEC, the overall migration reached  $34.8 \pm 4.6 \text{ mg dm}^{-2}$ . The increased migration in the case of the samples with 15 wt % TEC may be due to the excess of TEC in the hybrid

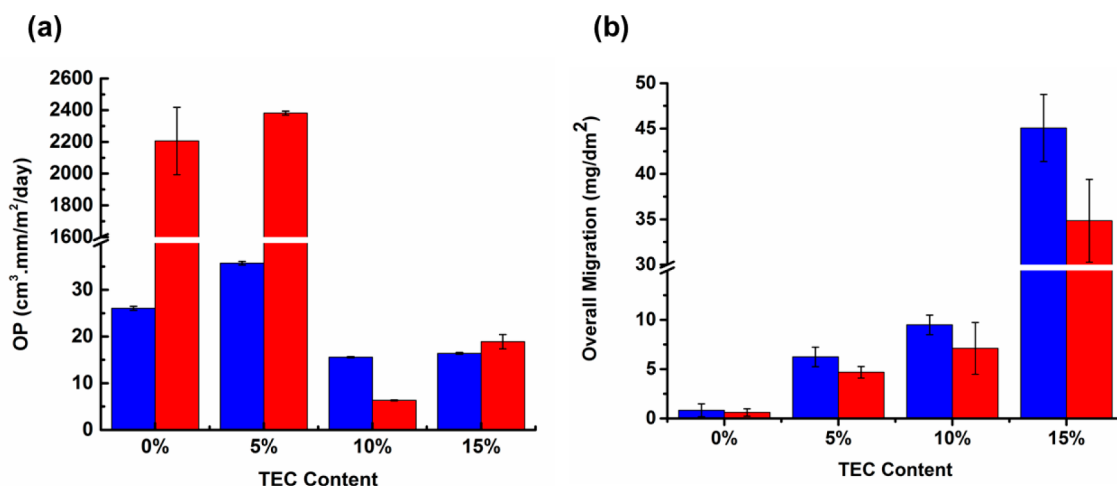


**Figure 8.** (a) Oxygen permeability properties of PLA, PLA/TEC, and all the developed PLA/MCC\_TEC biocomposites. The blue column represents PLA/TEC blends, and the red columns are their MCC-containing analogues. (b) Overall migration analysis of PLA/TEC and PLA/MCC\_TEC biocomposites. The blue column represents PLA/TEC blends, and the red columns are MCC-containing analogues.

systems after the extrusion and compression molding of film that may then migrate to the dry food simulant. TEC is not toxic, of natural origin, and FDA approved (21CFR 184.1911, EC commission directive 2007/19) as food contact material. Nevertheless, EU Regulation No. 10/2011 on plastic materials and articles has set an overall migration limit (OML) for any plastic food contact materials and articles to  $10 \text{ mg}/\text{dm}^2$ . For this reason, we propose the PLA/MCC\_10%TEC biocomposites for food packaging application.

**3.9. Ranking of the Developed Biocomposites Using TOPSIS.** TOPSIS analysis was used as the multicriteria decision-making (MCDM) tool for selecting the best possible PLA/MCC\_TEC biocomposites from the different blends and biocomposites presented in this study. The main aim of the TOPSIS method is to select the top-ranked biocomposite that is closest to the positive ideal solution and farthest from the negative ideal (hypothetically worst) solution. All the biocomposite materials have been compared following all the decision-making criteria as shown in Tables S2–S7. The relative closeness value to the ideal solution should always be in the  $0 \leq \text{relative closeness} \leq 1$  range. If the relative closeness is 1, the sample has the best solution conditions, whereas if the relative closeness is 0, the sample has the worst conditions.<sup>60</sup> The properties that were introduced in the decision matrix were tensile properties, water vapor permeability, oxygen permeability, and food migration, which are the most essential properties of materials developed for food packaging, and on the basis of these parameters, the ranking of PLA/MCC\_TEC biocomposites is shown in Figure 9. Although the PLA/MCC\_15%TEC biocomposite has been ranked in the first place, it could not be selected as the best solution due to its food migration value that is higher than the migration limit of  $10 \text{ mg}/\text{dm}^2$ . Since the PLA/MCC\_10%TEC biocomposite was ranked second, according to the TOPSIS evaluation, and its food migration levels are within the accepted limits, we propose it as the most suitable biocomposite for eco-friendly food packaging applications. The performance of PLA/MCC\_10%TEC is also compared to the performance of the other four packaging materials (i.e., LDPE, PP, EVOH, and PLA/Cacao films) using TOPSIS analysis (Figure S13 and Table S8, Supporting Information). According to the TOPSIS ranking, the PLA/MCC\_10%TEC biocomposite has reached

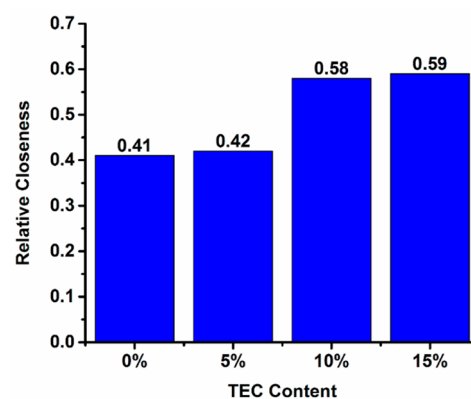


**Figure 9.** TOPSIS of the PLA/MCC\_TEC biocomposites. The TOPSIS analysis of PLA/TEC is shown in Figure S12.

the third position (ranking 3) even among the other materials. Therefore, in the pathway of developing new eco-friendly packaging materials, the TOPSIS analysis has proven that the PLA/MCC\_10%TEC biocomposite is a valuable candidate.

#### 4. CONCLUSIONS

In this study, we developed eco-friendly biocomposite formulations of PLA/MCC, plasticized with TEC, using extrusion followed by compression molding. The SEM and TGA analyses showed that the presence of TEC improves the compatibility and dispersion of the two biopolymers, resulting in improved water vapor and oxygen barrier properties. Using Tenax as a dry food simulant, we prove that the migration of molecules from the biocomposites remains below  $10 \text{ mg}/\text{dm}^2$  when the TEC concentration in the biocomposites is  $\leq 10 \text{ wt} \%$ , making them attractive for eco-friendly, cost-effective, and biobased food contact materials. According to the TOPSIS ranking of all the developed biocomposites, PLA/MCC\_10%TEC can be proposed as the most promising candidate for packaging applications, also concerning materials already present in the market.

## ■ ASSOCIATED CONTENT

### Supporting Information

The Supporting Information is available free of charge at <https://pubs.acs.org/doi/10.1021/acsapm.1c00281>.

Figures of SEM images, FTIR-ATR spectra, diffraction patterns, typical tensile stress–strain curves, deconvolution TGA spectra, thermal degradation behavior, dynamic water contact angles, moisture content analysis, OP values, TOPSIS analysis, and comparison of the performance analysis, discussions of FTIR-ATR analysis, SEM analysis, XRD analysis, tensile testing analysis, thermal degradation analysis, dynamic water contact angle, moisture content analysis, OP values of polymers, ranking of biocomposites using TOPSIS, and comparison of the performance of PLA/MCC\_10%TEC biocomposites by TOPSIS, and tables of main chemical functional groups biocomposites, decision matrix, normalization matrix, weight normalized matrix, ideal best and ideal worst solutions, separation measures, relative closeness value and ranking, and TOPSIS analysis data set (PDF)

## ■ AUTHOR INFORMATION

### Corresponding Author

Athanassia Athanassiou – Smart Materials, Istituto Italiano di Tecnologia, 16163 Genova, Italy; [orcid.org/0000-0002-6533-3231](https://orcid.org/0000-0002-6533-3231); Email: [athanassia.athanassiou@iit.it](mailto:athanassia.athanassiou@iit.it)

### Authors

Uttam C. Paul – Smart Materials, Istituto Italiano di Tecnologia, 16163 Genova, Italy; [orcid.org/0000-0002-0739-2727](https://orcid.org/0000-0002-0739-2727)

Despina Fragouli – Smart Materials, Istituto Italiano di Tecnologia, 16163 Genova, Italy; [orcid.org/0000-0002-2492-5134](https://orcid.org/0000-0002-2492-5134)

Ilker S. Bayer – Smart Materials, Istituto Italiano di Tecnologia, 16163 Genova, Italy; [orcid.org/0000-0002-7951-8851](https://orcid.org/0000-0002-7951-8851)

Arkadiusz Zych – Smart Materials, Istituto Italiano di Tecnologia, 16163 Genova, Italy

Complete contact information is available at: <https://pubs.acs.org/doi/10.1021/acsapm.1c00281>

### Notes

The authors declare no competing financial interest.

## ■ ACKNOWLEDGMENTS

The authors would like to acknowledge Lea Pasquale, Lara Marini, Materials Characterization Facility, and Istituto Italiano di Tecnologia for performing the XRD and TGA analyses.

## ■ REFERENCES

- (1) Huda, M. S.; Mohanty, A. K.; Drzal, L. T.; Schut, E.; Misra, M. Green composites from recycled cellulose and poly(lactic acid): Physico-mechanical and morphological properties evaluation. *J. Mater. Sci.* **2005**, *40* (16), 4221–4229.
- (2) Mihai, M.; Huneault, M. A.; Favis, B. D.; Li, H. Extrusion Foaming of Semi-Crystalline PLA and PLA/Thermoplastic Starch Blends. *Macromol. Biosci.* **2007**, *7* (7), 907–920.
- (3) Suryanegara, L.; Nakagaito, A. N.; Yano, H. The effect of crystallization of PLA on the thermal and mechanical properties of

microfibrillated cellulose-reinforced PLA composites. *Compos. Sci. Technol.* **2009**, *69* (7), 1187–1192.

(4) Mathew, A. P.; Oksman, K.; Sain, M. Mechanical properties of biodegradable composites from poly lactic acid (PLA) and microcrystalline cellulose (MCC). *J. Appl. Polym. Sci.* **2005**, *97* (5), 2014–2025.

(5) Oksman, K.; Mathew, A. P.; Bondeson, D.; Kvien, I. Manufacturing process of cellulose whiskers/poly(lactic acid) nanocomposites. *Compos. Sci. Technol.* **2006**, *66* (15), 2776–2784.

(6) Ljungberg, N.; Wesslén, B. The effects of plasticizers on the dynamic mechanical and thermal properties of poly(lactic acid). *J. Appl. Polym. Sci.* **2002**, *86* (5), 1227–1234.

(7) Vink, E. T.; Rábago, K. R.; Glassner, D. A.; Springs, B.; O'Connor, R. P.; Kolstad, J.; Gruber, P. R. The sustainability of NatureWorks polylactide polymers and Ingeo polylactide fibers: an update of the future. *Macromol. Biosci.* **2004**, *4* (6), 551–64.

(8) Johari, A. P.; Mohanty, S.; Kurmvanshi, S. K.; Nayak, S. K. Influence of Different Treated Cellulose Fibers on the Mechanical and Thermal Properties of Poly(lactic acid). *ACS Sustainable Chem. Eng.* **2016**, *4* (3), 1619–1629.

(9) Dai, X.; Xiong, Z.; Ma, S.; Li, C.; Wang, J.; Na, H.; Zhu, J. Fabricating Highly Reactive Bio-based Compatibilizers of Epoxidized Citric Acid To Improve the Flexural Properties of Polylactide/Microcrystalline Cellulose Blends. *Ind. Eng. Chem. Res.* **2015**, *54* (15), 3806–3812.

(10) Yang, Z.; Bi, H.; Bi, Y.; Rodrigue, D.; Xu, M.; Feng, X. Comparison between polyethylene glycol and tributyl citrate to modify the properties of wood fiber/poly(lactic acid) biocomposites. *Polym. Compos.* **2019**, *40* (4), 1384–1394.

(11) Fortunati, E.; Armentano, I.; Iannoni, A.; Barbale, M.; Zaccaro, S.; Scavone, M.; Visai, L.; Kenny, J. M. New multifunctional poly(lactide acid) composites: Mechanical, antibacterial, and degradation properties. *J. Appl. Polym. Sci.* **2012**, *124* (1), 87–98.

(12) Sabo, R.; Jin, L.; Stark, N.; Ibach, R. E. Effect of environmental conditions on the mechanical properties and fungal degradation of polycaprolactone/microcrystalline cellulose/wood flour composites. *BioResources* **2013**, *8* (3), 3322–3335.

(13) Mukherjee, T.; Sani, M.; Kao, N.; Gupta, R. K.; Quazi, N.; Bhattacharya, S. Improved dispersion of cellulose microcrystals in polylactic acid (PLA) based composites applying surface acetylation. *Chem. Eng. Sci.* **2013**, *101*, 655–662.

(14) Trifol, J.; Plackett, D.; Sillard, C.; Szabo, P.; Bras, J.; Daugaard, A. E. Hybrid poly(lactic acid)/nanocellulose/nanoclay composites with synergistically enhanced barrier properties and improved thermomechanical resistance. *Polym. Int.* **2016**, *65* (8), 988–995.

(15) Dhar, P.; Gaur, S. S.; Soundararajan, N.; Gupta, A.; Bhasney, S. M.; Milli, M.; Kumar, A.; Katiyar, V. Reactive Extrusion of Polylactic Acid/Cellulose Nanocrystal Films for Food Packaging Applications: Influence of Filler Type on Thermomechanical, Rheological, and Barrier Properties. *Ind. Eng. Chem. Res.* **2017**, *56* (16), 4718–4735.

(16) Jaratrotkamjorn, R.; Khaokong, C.; Tanrattanakul, V. Toughness enhancement of poly(lactic acid) by melt blending with natural rubber. *J. Appl. Polym. Sci.* **2012**, *124* (6), 5027–5036.

(17) Zhang, C.; Wang, W.; Huang, Y.; Pan, Y.; Jiang, L.; Dan, Y.; Luo, Y.; Peng, Z. Thermal, mechanical and rheological properties of polylactide toughened by epoxidized natural rubber. *Mater. Eng.* **2013**, *45*, 198–205.

(18) Wang, Y.; Wei, Z.; Li, Y. Highly toughened polylactide/epoxidized poly(styrene-*b*-butadiene-*b*-styrene) blends with excellent tensile performance. *Eur. Polym. J.* **2016**, *85*, 92–104.

(19) Feng, F.; Ye, L. Morphologies and mechanical properties of polylactide/thermoplastic polyurethane elastomer blends. *J. Appl. Polym. Sci.* **2011**, *119* (5), 2778–2783.

(20) Hong, H.; Wei, J.; Yuan, Y.; Chen, F.-P.; Wang, J.; Qu, X.; Liu, C.-S. A novel composite coupled hardness with flexibility—polylactic acid toughen with thermoplastic polyurethane. *J. Appl. Polym. Sci.* **2011**, *121* (2), 855–861.

(21) Peelman, N.; Ragaert, P.; Ragaert, K.; De Meulenaer, B.; Devlieghere, F.; Cardon, L. Heat resistance of new biobased

- polymeric materials, focusing on starch, cellulose, PLA, and PHA. *J. Appl. Polym. Sci.* **2015**, *132* (48), 42305.
- (22) Phuong, V. T.; Gigante, V.; Aliotta, L.; Coltelli, M.-B.; Cinelli, P.; Lazzeri, A. Reactively extruded eco-composites based on poly(lactic acid)/bisphenol A polycarbonate blends reinforced with regenerated cellulose microfibrils. *Compos. Sci. Technol.* **2017**, *139*, 127–137.
- (23) Siakeng, R.; Jawaid, M.; Ariffin, H.; Sapuan, S. M.; Asim, M.; Saba, N. Natural fiber reinforced polylactic acid composites: A review. *Polym. Compos.* **2019**, *40* (2), 446–463.
- (24) Kian, L. K.; Saba, N.; Jawaid, M.; Fouad, H. Characterization of microcrystalline cellulose extracted from olive fiber. *Int. J. Biol. Macromol.* **2020**, *156*, 347–353.
- (25) Zhang, Q.; Khan, M. U.; Lin, X.; Yi, W.; Lei, H. Green-composites produced from waste residue in pulp and paper industry: A sustainable way to manage industrial wastes. *J. Cleaner Prod.* **2020**, *262*, 121251.
- (26) Zhang, Q.; Lei, H.; Cai, H.; Han, X.; Lin, X.; Qian, M.; Zhao, Y.; Huo, E.; Villota, E. M.; Mateo, W. Improvement on the properties of microcrystalline cellulose/polylactic acid composites by using activated biochar. *J. Cleaner Prod.* **2020**, *252*, 119898.
- (27) Mohan Bhasney, S.; Kumar, A.; Katiyar, V. Microcrystalline cellulose, polylactic acid and polypropylene biocomposites and its morphological, mechanical, thermal and rheological properties. *Composites, Part B* **2020**, *184*, 107717.
- (28) Kian, L. K.; Saba, N.; Jawaid, M.; Sultan, M. T. H. A review on processing techniques of bast fibers nanocellulose and its polylactic acid (PLA) nanocomposites. *Int. J. Biol. Macromol.* **2019**, *121*, 1314–1328.
- (29) Xu, L.; Zhao, J.; Qian, S.; Zhu, X.; Takahashi, J. Green-plasticized poly(lactic acid)/nanofibrillated cellulose biocomposites with high strength, good toughness and excellent heat resistance. *Compos. Sci. Technol.* **2021**, *203*, 108613.
- (30) Supthanyakul, R.; Kaabuaathong, N.; Chirachanchai, S. Random poly(butylene succinate-co-lactic acid) as a multi-functional additive for miscibility, toughness, and clarity of PLA/PBS blends. *Polymers* **2016**, *105*, 1–9.
- (31) Singh, A. A.; Genovese, M. E.; Mancini, G.; Marini, L.; Athanassiou, A. Green Processing Route for Polylactic Acid-Cellulose Fiber Biocomposites. *ACS Sustainable Chem. Eng.* **2020**, *8* (10), 4128–4136.
- (32) Lee, M.; Jung, B. N.; Kim, G. H.; Kang, D.; Park, H. J.; Shim, J. K.; Hwang, S. W. The effect of triethyl citrate on the dispersibility and water vapor sorption behavior of polylactic acid/zeolite composites. *Polym. Test.* **2020**, *89*, 106571.
- (33) Ren, Z.; Dong, L.; Yang, Y. Dynamic mechanical and thermal properties of plasticized poly(lactic acid). *J. Appl. Polym. Sci.* **2006**, *101* (3), 1583–1590.
- (34) Harte, I.; Birkinshaw, C.; Jones, E.; Kennedy, J.; DeBarra, E. The effect of citrate ester plasticizers on the thermal and mechanical properties of poly(DL-lactide). *J. Appl. Polym. Sci.* **2013**, *127* (3), 1997–2003.
- (35) Mahmud, S.; Long, Y.; Abu Taher, M.; Xiong, Z.; Zhang, R.; Zhu, J. Toughening polylactide by direct blending of cellulose nanocrystals and epoxidized soybean oil. *J. Appl. Polym. Sci.* **2019**, *136* (46), 48221.
- (36) Clarkson, C. M.; El Awad Azrak, S. M.; Schueneman, G. T.; Snyder, J. F.; Youngblood, J. P. Crystallization kinetics and morphology of small concentrations of cellulose nanofibrils (CNFs) and cellulose nanocrystals (CNCs) melt-compounded into poly(lactic acid) (PLA) with plasticizer. *Polymer* **2020**, *187*, 122101.
- (37) Labrecque, L. V.; Kumar, R. A.; Davé, V.; Gross, R. A.; McCarthy, S. P. Citrate esters as plasticizers for poly(lactic acid). *J. Appl. Polym. Sci.* **1997**, *66* (8), 1507–1513.
- (38) Maiza, M.; Benaniba, M. T.; Quintard, G.; Massardier-Nageotte, V. Biobased additive plasticizing Polylactic acid (PLA). *Polim.: Cienc. Tecnol.* **2015**, *25*, 581–590.
- (39) Shirai, M. A.; Grossmann, M. V. E.; Mali, S.; Yamashita, F.; Garcia, P. S.; Müller, C. M. O. Development of biodegradable flexible films of starch and poly(lactic acid) plasticized with adipate or citrate esters. *Carbohydr. Polym.* **2013**, *92* (1), 19–22.
- (40) Park, H.-M.; Misra, M.; Drzal, L. T.; Mohanty, A. K. Green Nanocomposites from Cellulose Acetate Bioplastic and Clay: Effect of Eco-Friendly Triethyl Citrate Plasticizer. *Biomacromolecules* **2004**, *5* (6), 2281–2288.
- (41) Singh, A. A.; Sharma, S.; Srivastava, M.; Majumdar, A. Modulating the properties of polylactic acid for packaging applications using biobased plasticizers and naturally obtained fillers. *Int. J. Biol. Macromol.* **2020**, *153*, 1165–1175.
- (42) Singh, S.; Maspoch, M. L.; Oksman, K. Crystallization of triethyl-citrate-plasticized poly(lactic acid) induced by chitin nanocrystals. *J. Appl. Polym. Sci.* **2019**, *136* (36), 47936.
- (43) Xiao, L.; Mai, Y.; He, F.; Yu, L.; Zhang, L.; Tang, H.; Yang, G. Bio-based green composites with high performance from poly(lactic acid) and surface-modified microcrystalline cellulose. *J. Mater. Chem.* **2012**, *22* (31), 15732–15739.
- (44) Xu, A.; Wang, F. Carboxylate ionic liquid solvent systems from 2006 to 2020: thermal properties and application in cellulose processing. *Green Chem.* **2020**, *22* (22), 7622–7664.
- (45) Xu, A.; Wang, Y.; Gao, J.; Wang, J. Facile fabrication of a homogeneous cellulose/polylactic acid composite film with improved biocompatibility, biodegradability and mechanical properties. *Green Chem.* **2019**, *21* (16), 4449–4456.
- (46) Fortunati, E.; Armentano, I.; Iannoni, A.; Kenny, J. M. Development and thermal behaviour of ternary PLA matrix composites. *Polym. Degrad. Stab.* **2010**, *95* (11), 2200–2206.
- (47) Herrera, N.; Salaberria, A. M.; Mathew, A. P.; Oksman, K. Plasticized polylactic acid nanocomposite films with cellulose and chitin nanocrystals prepared using extrusion and compression molding with two cooling rates: Effects on mechanical, thermal and optical properties. *Composites, Part A* **2016**, *83*, 89–97.
- (48) Joseph, S.; Deenadayalan, E.; Mahanwar, P. A. Studies on Melt Processable Biocomposites of Polylactic Acid. *J. Polym. Environ.* **2015**, *23* (3), 321–333.
- (49) Mathew, A. P.; Oksman, K.; Sain, M. The effect of morphology and chemical characteristics of cellulose reinforcements on the crystallinity of polylactic acid. *J. Appl. Polym. Sci.* **2006**, *101* (1), 300–310.
- (50) Santos, F. A. d.; Tavares, M. I. B. Development and characterization of hybrid materials based on biodegradable PLA matrix, microcrystalline cellulose and organophilic silica. *Polim.: Cienc. Tecnol.* **2014**, *24*, 561–566.
- (51) Haafiz, M. K. M.; Hassan, A.; Zakaria, Z.; Inuwa, I. M.; Islam, M. S.; Jawaid, M. Properties of polylactic acid composites reinforced with oil palm biomass microcrystalline cellulose. *Carbohydr. Polym.* **2013**, *98* (1), 139–145.
- (52) Dogu, B.; Kaynak, C. Behavior of polylactide/microcrystalline cellulose biocomposites: effects of filler content and interfacial compatibilization. *Cellulose* **2016**, *23* (1), 611–622.
- (53) Xu, A.; Chen, L.; Wang, J. Functionalized Imidazolium Carboxylates for Enhancing Practical Applicability in Cellulose Processing. *Macromolecules* **2018**, *51* (11), 4158–4166.
- (54) Frone, A. N.; Berlioz, S.; Chailan, J. F.; Panaitescu, D. M.; Donescu, D. Cellulose fiber-reinforced polylactic acid. *Polym. Compos.* **2011**, *32* (6), 976–985.
- (55) Papadopoulou, E. L.; Paul, U. C.; Tran, T. N.; Suarato, G.; Ceseracciu, L.; Marras, S.; D'Arcy, R.; Athanassiou, A. Sustainable Active Food Packaging from Poly(lactic acid) and Cocoa Bean Shells. *ACS Appl. Mater. Interfaces* **2019**, *11* (34), 31317–31327.
- (56) Ho, T. T. T.; Zimmermann, T.; Ohr, S.; Caseri, W. R. Composites of Cationic Nanofibrillated Cellulose and Layered Silicates: Water Vapor Barrier and Mechanical Properties. *ACS Appl. Mater. Interfaces* **2012**, *4* (9), 4832–4840.
- (57) Tran, T. N.; Paul, U.; Heredia-Guerrero, J. A.; Liakos, I.; Marras, S.; Scarpellini, A.; Ayadi, F.; Athanassiou, A.; Bayer, I. S. Transparent and flexible amorphous cellulose-acrylic hybrids. *Chem. Eng. J.* **2016**, *287*, 196–204.

(58) Perotto, G.; Ceseracciu, L.; Simonutti, R.; Paul, U. C.; Guzman-Puyol, S.; Tran, T.-N.; Bayer, I. S.; Athanassiou, A. Bioplastics from vegetable waste via an eco-friendly water-based process. *Green Chem.* **2018**, *20* (4), 894–902.

(59) Paul, U. C.; Fragouli, D.; Bayer, I. S.; Mele, E.; Conchione, C.; Cingolani, R.; Moret, S.; Athanassiou, A. Mineral oil barrier sequential polymer treatment for recycled paper products in food packaging. *Mater. Res. Express* **2017**, *4* (1), 015501.

(60) Khorshidi, R.; Hassani, A. Comparative analysis between TOPSIS and PSI methods of materials selection to achieve a desirable combination of strength and workability in Al/SiC composite. *Mater. Eng.* **2013**, *52*, 999–1010.

(61) Patel, V. K.; Rawat, N. Physico-mechanical properties of sustainable Sagwan-Teak Wood Flour/Polyester Composites with/without gum rosin. *Sustainable Mater. Technol.* **2017**, *13*, 1–8.

(62) Herrera, N.; Singh, A. A.; Salaberria, A. M.; Labidi, J.; Mathew, A. P.; Oksman, K. Triethyl Citrate (TEC) as a Dispersing Aid in Poly(lactic acid)/Chitin Nanocomposites Prepared via Liquid-Assisted Extrusion. *Polymers* **2017**, *9* (12), 406.

(63) Qu, P.; Gao, Y.; Wu, G.; Zhang, L. Nanocomposites of poly(lactic acid) reinforced with cellulose nanofibrils. *BioRes.* **2010**, *5* (3), 1811–1823.

(64) Ke, T.; Sun, X. S. Thermal and mechanical properties of poly(lactic acid)/starch/methylenediphenyl diisocyanate blending with triethyl citrate. *J. Appl. Polym. Sci.* **2003**, *88* (13), 2947–2955.

(65) Karkhanis, S. S.; Stark, N. M.; Sabo, R. C.; Matuana, L. M. Water vapor and oxygen barrier properties of extrusion-blown poly(lactic acid)/cellulose nanocrystals nanocomposite films. *Composites, Part A* **2018**, *114*, 204–211.

(66) Gupta, A.; Katiyar, V. Cellulose Functionalized High Molecular Weight Stereocomplex Poly(lactic acid) Biocomposite Films with Improved Gas Barrier, Thermomechanical Properties. *ACS Sustainable Chem. Eng.* **2017**, *5* (8), 6835–6844.

(67) Zhang, X.; Zhu, W.; He, G.; Zhang, P.; Zhang, Z.; Parkin, I. P. Flexible and mechanically robust superhydrophobic silicone surfaces with stable Cassie-Baxter state. *J. Mater. Chem. A* **2016**, *4* (37), 14180–14186.

(68) Wang, J.; Gardner, D. J.; Stark, N. M.; Bousfield, D. W.; Tajvidi, M.; Cai, Z. Moisture and Oxygen Barrier Properties of Cellulose Nanomaterial-Based Films. *ACS Sustainable Chem. Eng.* **2018**, *6* (1), 49–70.